



Published in final edited form as:

Otolaryngol Head Neck Surg. 2019 September ; 161(3): 458–467. doi:10.1177/0194599819844754.

Factors Influencing Poor Outcomes in Synthetic Tissue-Engineered Tracheal Replacement

Victoria Pepper, MD¹, Cameron A. Best^{2,3}, Kaila Buckley, MD⁴, Cynthia Schwartz, MD, MS⁵, Ekene Onwuka, MD, MS⁶, Nakesha King, MD, MS⁶, Audrey White⁷, Sayali Dharmadhikari, MS^{2,8}, Susan D. Reynolds, PhD⁹, Jed Johnson, PhD¹⁰, Jonathan Grischkan, MD⁸, Christopher K. Breuer, MD^{2,11}, Tendy Chiang, MD^{2,8}

¹Division of Pediatric Surgery, Loma Linda Children's Hospital, Loma Linda, California, USA

²Center for Regenerative Medicine, Research Institute at Nationwide Children's Hospital, Columbus, Ohio, USA

³Biomedical Sciences Graduate Program, College of Medicine, The Ohio State University, Columbus, Ohio, USA

⁴Department of Pathology, The Ohio State University, Columbus, Ohio, USA

⁵Department of Otolaryngology, Texas Tech University Health Sciences Center, Lubbock, Texas, USA

⁶Department of General Surgery, The Ohio State University, Columbus, Ohio, USA

⁷College of Medicine, The Ohio State University, Columbus, Ohio, USA

Reprints and permission: sagepub.com/journalsPermissions.nav

Corresponding Author: Tendy Chiang, MD, Nationwide Children's Hospital, 555 S 18th St, Ste 2A, Columbus, OH 43205-2664, USA. tendy.chiang@nationwidechildrens.org

Author Contributions

Victoria Pepper, study design, acquisition, analysis, interpretation of data, drafting and revising content, provided final approval of the version to be published, agrees to be accountable for all aspects of work; **Cameron Best**, study design, acquisition, analysis, interpretation of data, drafting and revising content, provided final approval of the version to be published, agrees to be accountable for all aspects of work; **Kaila Buckley**, interpretation of data, drafting and revising content, provided final approval of the version to be published, agrees to be accountable for all aspects of work; **Cynthia Schwartz**, interpretation of data, drafting and revising content, provided final approval of the version to be published, agrees to be accountable for all aspects of work; **Ekene Onwuka**, interpretation of data, drafting and revising content, provided final approval of the version to be published, agrees to be accountable for all aspects of work; **Nakesha King**, interpretation of data, drafting and revising content, provided final approval of the version to be published, agrees to be accountable for all aspects of work; **Audrey White**, interpretation of data, drafting and revising content, provided final approval of the version to be published, agrees to be accountable for all aspects of work; **Sayali Dharmadhikari**, interpretation of data, drafting and revising content provided final approval of the version to be published, agrees to be accountable for all aspects of work; **Susan D. Reynolds**, interpretation of data, drafting and revising content, provided final approval of the version to be published, agrees to be accountable for all aspects of work; **Jed Johnson**, study design, acquisition, analysis, interpretation of data, drafting and revising content, provided final approval of the version to be published, agrees to be accountable for all aspects of work; **Jonathan Grischkan**, study design, acquisition, analysis, interpretation of data, drafting and revising content, provided final approval of the version to be published, agrees to be accountable for all aspects of work; **Christopher Breuer**, study design, acquisition, analysis, interpretation of data, drafting and revising content provided final approval of the version to be published, agrees to be accountable for all aspects of work; **Tendy Chiang**, study design, acquisition, analysis, interpretation of data, drafting and revising content, provided final approval of the version to be published, agrees to be accountable for all aspects of work.

Disclosures

Competing interests: Cameron Best, consultant, cofounder with equity stake, and patent owner of LYST Therapeutics, LLC; Jed Johnson, Nanofiber Solutions—salary, equity, intellectual property, and cofounder; fabricated the grafts used in the study; Christopher Breuer, Cook Biomedical—scientific advisory board; LYST Therapeutics, LLC—cofounder, stock, intellectual property; Gunze Limited—grant support; Cook Regentec/Pall Corp—grant support/intellectual property; Food and Drug Administration, National Institutes of Health, University of Washington—advisory board.

Sponsorships: None.

⁸Department of Otolaryngology–Head and Neck Surgery, Nationwide Children’s Hospital, Columbus, Ohio, USA

⁹Center for Perinatal Research, Research Institute at Nationwide Children’s Hospital, Columbus, Ohio, USA

¹⁰Nanofiber Solutions Inc, Hilliard, Ohio, USA

¹¹Department of Pediatric Surgery, Nationwide Children’s Hospital, Columbus, Ohio, USA

Abstract

Objectives.—Humans receiving tissue-engineered tracheal grafts have experienced poor outcomes ultimately resulting in death or the need for graft explantation. We assessed the performance of the synthetic scaffolds used in humans with an ovine model of orthotopic tracheal replacement, applying standard postsurgical surveillance and interventions to define the factors that contributed to the complications seen at the bedside.

Study Design.—Large animal model.

Setting.—Pediatric academic research institute.

Subjects and Methods.—Human scaffolds were manufactured with an electrospun blend of polyethylene terephthalate and polyurethane reinforced with polycarbonate rings. They were seeded with autologous bone marrow–derived mononuclear cells and implanted in sheep. Animals were evaluated with routine bronchoscopy and fluoroscopy. Endoscopic dilation and stenting were performed to manage graft stenosis for up to a 4-month time point. Grafts and adjacent native airway were sectioned and evaluated with histology and immunohistochemistry.

Results.—All animals had signs of graft stenosis. Three of 5 animals (60%) designated for long-term surveillance survived until the 4-month time point. Graft dilation and stent placement resolved respiratory symptoms and prolonged survival. Necropsy demonstrated evidence of infection and graft encapsulation. Granulation tissue with signs of neovascularization was seen at the anastomoses, but epithelialization was never observed. Acute and chronic inflammation of the native airway epithelium was observed at all time points. Architectural changes of the scaffold included posterior wall infolding and scaffold delamination.

Conclusions.—In our ovine model, clinically applied synthetic tissue-engineered tracheas demonstrated infectious, inflammatory, and mechanical failures with a lack of epithelialization and neovascularization.

Keywords

tissue engineering; trachea; regenerative medicine; biomaterials; stem cells

In the last decade, the lack of surgical options to treat long-segment tracheal defects had accelerated human implantation of tissue-engineered tracheal grafts (TETGs).^{1–4} Initial reported success propelled the introduction of synthetic scaffolds to spare the need for donor tissue. However, human outcomes with synthetic tracheal replacement have been fraught with complications, including stenosis, delayed epithelialization, the need for explantation, and death.^{1,3–8} In addition, inquiries in clinical reports have emphasized the need for further

preclinical testing.^{9,10} Given the challenges of characterizing outcomes in human recipients, we used a lamb model of orthotopic implantation of synthetic TETGs to further define the complications seen at the bedside.

Previous studies suggested that seeding synthetic tracheal scaffolds with autologous bone marrow–derived mononuclear cells (BM-MNCs) attenuates stenosis and accelerates graft epithelialization.¹¹ We noted that, similar to complications of open airway surgery, stenosis of TETGs was the predominant morbidity observed, resulting in airway obstruction, respiratory distress, and animal mortality. We demonstrated that bronchoscopic interventions such as balloon dilation and stenting can be used to palliate stenosis.¹² The aim of this study was to describe histologic and clinical outcomes with consistent postimplantation surveillance and interventions for TETGs to define both long-term regenerative outcomes and the modes of graft failure.

Methods

Animal Care and Ethics Statement

The Institutional Animal Care and Use Committee of Nationwide Children's Hospital approved the protocol (AR13–00071). Animal care was provided in accordance with humane care standards published by the Public Health Service in the *Care and Use of Laboratory Animals* (2011; National Institutes of Health, Bethesda, Maryland) and US Department of Agriculture regulations outlined in the Animal Welfare Act.

Scaffold Fabrication.—Scaffolds were manufactured as previously described.^{12–14} Briefly, 20% polyethylene terephthalate (PET) and 80% polyurethane (PU) polymer nanofiber precursor solutions were electrospun on a custom mandrel. Tracheal rings were 3-dimensionally (3D) printed from medical-grade polycarbonate and embedded into the graft during electrospinning, producing a 5-ringed scaffold that was 70 mm long with a 20-mm inner diameter and 22-mm outer diameter. Excess length to secure the graft to the mandrel for cell seeding was ultimately trimmed to a functional graft of 50 mm for implantation. Scaffolds were sterilized with 35 kGy of gamma irradiation.

Scaffold Characterization.—Scaffolds were mounted, gold sputter coated, and imaged with scanning electron microscopy. With ImageJ software (National Institutes of Health, Bethesda, Maryland), the mean \pm SD pore diameter was 5.4 ± 2.0 μm , and the mean fiber diameter was 1.0 ± 0.58 μm . Per ISO standard 7198 (second edition, 2016-08-01), the porosity was calculated as $75.72\% \pm 1.04\%$. The pores were completely interconnected, and the fibers were not point bonded.

Representative scaffolds ($n = 5$) were mechanically tested separately in medial-lateral and anterior-posterior compression with a servohydraulic materials test frame as previously described (858 Bionix; MTS Corp, Eden Prairie, Minnesota).¹⁴ Compression to 75% luminal narrowing demonstrated a maximum load of 32.8 ± 0.38 N (medial-lateral) and 104.4 ± 1.75 N (anterior-posterior). There was no evidence of graft delamination or design failure during mechanical testing.

Bone Marrow Harvest, BM-MNC Enrichment, and TETG Scaffold Seeding.—

Bone marrow harvest, BM-MNC enrichment with graft seeding, and implantation were performed during a single surgical intervention. Juvenile sheep (Dorset, *Ovisaries*, n = 8, 41 ± 10.5 kg) were first given butorphanol/midazolam (0.2/0.5 mg/kg intramuscular), and general anesthesia was then induced with ketamine (5–10 mg/kg) with diazepam (0.02–0.08 mg/kg) or propofol (4 mg/kg). Anesthesia was maintained with isoflurane (1%–5% in oxygen) and/or propofol (20–40 mg/kg/h).

In a sterile fashion, a 1-cm incision was made over the iliac crest, and a Jamshidi needle (Carefusion Inc, Franklin Lakes, New Jersey) was used to cannulate the marrow space (Figure 1A, A.1). A target volume of 5 mL/kg of bone marrow was aspirated into syringes containing heparinized saline.

BM-MNCs were enriched from heparinized bone marrow with a disposable closed-filtration system (Pall Corporation, Port Washington, New York) via size exclusion under gravity filtration (Figure 1B).^{15–19} The PET/PU scaffold was then secured to a fenestrated mandrel and submerged in BM-MNCs and vacuum seeded (–5 to –10 mm Hg; Figure 1C).^{13,14} Samples of the graft were obtained for DNA assay. Pre- and postseeding BM-MNC suspensions were sampled for manual and automated cell counts. Our prior experience established that no gross morphologic or mechanical alterations to the synthetic scaffold occur during this process.^{14,18,20}

DNA Assay and Determination of Seeding Efficiency.—Cell seeding efficiency was quantified via manual hemocytometer or automated cell count (Countess Automated Cell Counter; Fisher Scientific, Waltham, Massachusetts). Double-stranded DNA content in seeded scaffold samples (n = 4, 5 × 5-mm³ samples per graft) was determined via fluorimetric assay (QuantiT PicoGreen dsDNA Assay; Life Technologies, Carlsbad, California) per the manufacturer's protocol as previously described.^{14,21} Preseeding suspensions or graft sections were frozen in dH₂O overnight at –80°C to induce cell lysis. PicoGreen reagent was added to 50 µL of the thawed sample and incubated for 3 minutes at room temperature prior to measurement of fluorescence with a SpectraMax M5 spectrophotometer (excitation: 480 nm, emission: 520 nm; Molecular Devices, San Jose, California). Density of cell seeding (cells/mm³) was interpolated from a standard curve of an aliquot of the preseeding suspension assayed in parallel and reported as box plots with median lines and minimum, maximum values (Figure 2).

TETG Implantation.—During BM-MNC enrichment and scaffold seeding, the animal was placed in a supine position. Preoperative bronchoscopy was performed, and the site of graft implantation was measured with endoscopic techniques (Figure 1D.1).²² Radiographic assessment was then performed with 3D fluoroscopy producing axial, sagittal, and coronal images of the trachea equivalent to computed tomography (Figure 1D.2).

Animals were given intra- and postoperative antibiotics (cefazolin, 50 mg/kg/d) for 1 week. Through a vertical mid-line incision, a 5-cm segment of native trachea was isolated and resected (Figure 1D.3). The seeded TETG was then orthotopically implanted with interrupted 3–0 polydioxanone suture (PDS; Ethicon, Somerville, New Jersey). Implantation

was oriented in an interposition fashion with direct opposition of the lumen of the scaffold with the native airway lumen (Figure 1E.1). Postoperative rigid bronchoscopy and imaging (3D fluoroscopy) were obtained (Figure 1E.2–4). Surgical clips were placed to radiographically define the anastomoses (Figure 1E.2).

Postimplantation Surveillance.—Animals were extubated immediately after surgery. They were monitored for signs of respiratory distress and pain. Veterinary staff independently monitored the health of the sheep in accordance with current practices and standards for laboratory animal husbandry.

With use of clinical respiratory distress scales as previously described, clinical symptoms were observed on a daily basis (stridor, tachypnea, retractions, increased work of breathing, hypoxia, cyanosis, wheezing, cough).²³ Respiratory symptom scores were assigned in addition to standard measures of animal health. The initial study endpoint was 6 weeks; this was extended to 4 months when feasibility of endoscopic interventions was demonstrated (animals 4–8; Table 1). Surveillance bronchoscopy and 3D fluoroscopy were performed at 3 weeks, 6 weeks, 3 months, and 4 months. Graft lumen size and the grade of stenosis were defined with the Cotton-Myer scale.^{22,24} Emergent airway intervention with balloon dilation and stent placement was performed for graft stenosis and respiratory distress (Figure 1F, G). These procedures were performed under general anesthesia with spontaneous ventilation. Graft dilation was performed in response to stenosis .50% of luminal area at any level of the graft. Balloon dilation of the stenotic regions was performed with 14- to 16-mm airway balloons inflated to 8 to 10 atm for 1 minute (Acclarent, Irvine, California). When the plane of anesthesia did not permit balloon dilation due to hypoxia, serial dilation was performed with sequential placement of endotracheal tubes (sizes, 8.5–10). Graft patency was maintained with placement of a silicone stent (Hood Laboratories, Pembroke, Massachusetts) with a Pilling Jackson Alligator forceps (Teleflex, North Carolina) and confirmed with bronchoscopy.

Euthanasia and Necropsy.—Planned euthanasia endpoints were 6 weeks (n = 3) and 4 months (n = 5). At this point or as determined by clinical decision making of animal condition, animals were administered an overdose cocktail of ketamine (20–40 mg/kg, intravenous). After confirmation of deep sedation via absence of pupillary light response, animals were euthanized via bilateral pneumothoraces, exsanguination, and harvest of vital organs. Vital organs were weighed, evaluated for gross pathology, and formalin fixed.

Histologic Analysis.—TETG and native trachea proximal and distal to the graft were fixed in 10% neutral buffered formalin (Fisher Scientific) at 4°C overnight and then transferred to 70% EtOH. Segments of the host trachea and graft were divided for paraffin, glycolmethacrylate, or methylmethacrylate embedding (Figure 3). Slides were prepared (4-mm-thick serial sections) and stained with hematoxylin and eosin and Lee's methylene blue for paraffin and resin embedded sections, respectively. Slides were imaged on a Zeiss Axio Observer Z.1 microscope, and photomicrographs were acquired with a Zeiss AxioCam 105 camera at 2×, 10×, 20×, and 40× magnifications. Interpretation was performed by a pathologist (K.B.).

Immunohistochemistry.—Slides were deparaffinized with xylene and rehydrated with a graded ethanol series. Antigen retrieval was performed, and specimens were blocked prior to incubation with primary antibodies. Primary antibodies included CD68 (1:250 dilution ratio; Abcam, Cambridge, Massachusetts) and α -SMA (α -smooth muscle actin, 1:2000 dilution ratio; Dako, Carpinteria, California). Antibody binding was detected with appropriate biotinylated secondary antibodies (Vector Laboratories, Burlingame, California), followed by binding of streptavidin-horseradish peroxidase (Vector Laboratories) and color development with 3,3-diaminobenzidine (Vector Laboratories).

Results

PET/PU Tracheal Scaffolds Can Be Seeded with Autologous BM-MNCs

A consistent bone marrow volume of 5.07 ± 0.08 mL/kg (207.7 ± 52.2 mL) was aspirated from each animal. Preseeding cell viability and seeding efficiency were consistent and favorable ($74\% \pm 14\%$ and $57\% \pm 15\%$, respectively). Despite precision in harvested bone marrow, dsDNA assay results had variable cell seeding results ($7.46 \times 10^5 \pm 3.86 \times 10^5$ cells/mm³; Figure 2A), suggesting high variability in cellular concentration between hosts.

BM-MNC Harvest/Isolation, Graft Seeding, and Orthotopic Tracheal Replacement with Synthetic TETG Can Be Performed as 1 Surgical Intervention

A total of 8 animals underwent bone marrow harvest, BM-MNC isolation, graft seeding, and orthotopic tracheal replacement. Mean operative time was 4.88 ± 0.98 hours. All sheep tolerated the procedure well and were extubated on postoperative day 0. While BM-MNC isolation and graft seeding were performed, the animal underwent repositioning for implant and airway assessment with bronchoscopy and 3D fluoroscopy. Exposure of the cervical trachea was then achieved, and the seeded graft was orthotopically implanted. There were no intraoperative delays or complications.

Poor BM-MNC Seeding Correlates with Early Presentation of Respiratory Distress

There was a correlation between the density of seeded cells and severity of respiratory symptoms (Figure 2B). DNA assay results for each graft were plotted against earliest presentation of respiratory symptoms (prior to endoscopic intervention) and worst respiratory symptom score (regardless of prior intervention). Lower seeded cell dose correlated with earlier presentation of respiratory symptoms ($P = .0188$). There was no correlation between cell dose and the worst respiratory symptom score.

Respiratory Distress Evolves within Weeks of Implantation and Represents Fixed Stenosis of the Graft at the Anastomoses

The postoperative course is summarized in Table 1. Onset of respiratory distress presented on postoperative day 18 ± 7 , most commonly manifesting as stridor ($n = 6$). Progression of respiratory distress led to emergent intervention in 2 cases prior to the first scheduled surveillance bronchoscopy (Figure 1H–M). Of note, these 2 animals were the smallest animals with the greatest mismatch of native airway to graft size.

The first bronchoscopy demonstrated evidence of graft stenosis in all animals. Fluoroscopic 3D reconstructions confirmed that stenosis was most evident at the proximal and distal anastomosis, histologically characterized by exuberant granulation tissue (Figure 3A, B). Bronchoscopic and radiographic surveillance raised concerns that scaffold architecture was commonly distorted, presenting with infolding of the posterior tracheal wall and with scaffold delamination, which was confirmed on histopathologic analysis (Figure 3C, D).

Graft Stenosis Can Be Successfully Managed with Endoscopic Interventions Permitting Assessment of Long-term Graft Performance

Tracheal dilation with stent placement resulted in resolution of graft stenosis and respiratory distress. Responsiveness to endoscopic interventions leads to extension of the terminal endpoint to 4 months (Table 1). Despite improvement in clinical symptoms and prolonged survival, this did not result in improved graft epithelialization.

Gross Sections Illustrate Modes of Synthetic TETG Failure

The analysis of gross pathology revealed that graft failure occurred in multiple modes (Figure 4). Mechanical failure was present due to graft delamination (Figures 3D and 4) and posterior wall infolding (Figures 3C and 4). Infection, fibrinopurulent exudate, and excessive granulation tissue formation were present. Specimens lacked signs of substantial epithelial migration or viable neotissue formation.

Graft-Related Neotissue Resembles Granulation Tissue with Foreign Body Reaction

Neotissue was limited to the anastomosis and adjacent to the graft. Extraluminal tissue showed signs of fibrosis and neovascularization. There was no histologic evidence of neovascularization within the scaffold. Neotissue was not observed within the midgraft region. Graft-related neotissue was histologically characteristic of granulation tissue. Fibroblasts and CD68+ macrophages with multinucleated giant cells were surrounded by regions of neovascularization (Figure 5A–C). Vascularity (α -SMA1 vessels) was increased in graft-related neotissue (Figure 5D) as compared with native trachea tissue.

Persistent Inflammation within the Native Trachea May Contribute to Failure of Host Epithelial Migration

Native trachea adjacent to the TETG at the time of necropsy was compared with the excised tracheal segment at the time of graft implantation (Figure 6). Tracheal sections distal to the anastomosis showed signs of inflammation with increased nuclear density, cellularity, and disrupted architecture. Macrophage (CD68+) infiltration was observed in native tissue adjacent to the graft and graft-related neotissue at early time points following graft implantation and persisted at late time points (Figure 5C, 5C.1). Disruption of epithelial topography (papillary infolding) was present and more exaggerated at late-time point specimens (Figure 6C, D). Lamina propria thickening, increased nuclear density, cellularity, and glandular hyperplasia were all observed.

Lung Infection Is Commonly Found at Necropsy

Two animals were euthanized at the 3-week time point. One demonstrated progressive respiratory distress following bronchoscopy with dilation and had right upper lobe pneumonia, and 1 had an anesthesia-related complication during bronchoscopy that required euthanasia. Two animals were euthanized at the 6-week time point. One had an anesthesia-related complication during bronchoscopy. The second was hypoxic during bronchoscopy and had a lung abscess and pneumonia upon necropsy. One animal demonstrated complete graft dislodgment at the 3-month bronchoscopy and was euthanized upon development of respiratory distress 4 days later. Bronchoscopy showed graft encapsulation with a sleeve of malacic soft tissue contiguous with the native trachea. The remaining 3 animals were euthanized at the 4-month time point, with 1 noted to have a lung abscess.

Discussion

In 2008, the first TETG was implanted in a human recipient with decellularized trachea to replace a diseased left mainstem bronchus.²⁵ Additional implants for tracheal replacement were then performed in humans with poor outcomes.^{2-4,6,7,26-28} To spare the need for donor tissue, the first synthetic tracheal scaffold was implanted in a human recipient in 2011.²⁹ Of the human recipients of synthetic TETGs implanted, all are deceased or required graft explantation.^{6-8,28,30} To evaluate the limitations in synthetic tracheal replacement, we studied the synthetic scaffold used in prior clinical and preclinical studies with a lamb model.^{13,31} This model was selected because sheep are naturally outbred and genetically diverse; they have similar respiratory histologic, anatomic, and physiologic properties; they are used to model pulmonary disease in humans; and they have served as a preclinical foundation for the study of tissue-engineered vascular grafts.³²⁻³⁴ In a pilot study, we identified that graft stenosis is the predominant complication seen and that it is responsive to endoscopic dilation and stent placement.¹²

In this study, we categorized failure of TETGs into infectious, mechanical, and inflammatory missteps, ultimately resulting in inadequate neotissue formation. We hypothesize that this is a result of delayed epithelialization and poor blood supply. Despite graft seeding, implantation of a nonvascularized, nonepithelialized graft results in a large defect in the mucociliary ladder that increases the risk of infection, inflammation, and graft encapsulation.

Half of the animals demonstrated infectious processes within the lung parenchyma manifesting as lung abscess (n = 3) and pneumonia (n = 1) at the time of necropsy (Figure 7B). On gross analysis, fibropurulent exudate was noted directly around the graft in all specimens. Intraluminal purulence was seen at the time of initial bronchoscopy in all animals (Figure 7A). Infectious complications led to intraoperative hypoxia requiring euthanasia in at least 1 case. One factor that is important in preventing infectious failure is the development of a functional epithelium. Our preliminary study identified the migration of epithelium at the anastomoses, suggesting that a longer study interval could lead to further graft epithelialization.¹¹ However, there was no progression of graft epithelialization at our latest surveillance time point of 4 months.

With any tissue-engineered scaffold, the biomechanics of the scaffold interacting with the native tissues play an important role in the success or failure of a graft. A tracheal scaffold must maintain integrity against static tensile forces, dynamic respiratory forces, neck movements, and wound contracture after implantation. Conversely, supraphysiologic scaffold properties create compliance mismatch, which can result in graft stenosis or failure.^{35–37} The synthetic scaffold that we assessed was designed to have mechanical properties similar to native trachea.¹⁴ Even with optimization of mechanical compatibility, all grafts demonstrated stenosis, delamination, and posterior wall infolding (Figure 7C–F).

Currently, there is no consensus on the ideal scaffold composition for tracheal tissue engineering. Decellularized tissue is nonimmunogenic but requires a donor and relies on host integration to maintain graft integrity.^{38–40} Allograft materials may not demonstrate the same mechanical properties as native trachea and have required immunosuppression.^{26,41} While synthetic materials can be easily customized, they can lead to chronic inflammation and infection. Animal models comparing these approaches demonstrated evidence of graft compromise, with the majority of graft recipients requiring early termination prior to 30 days.⁴⁰ Recent clinical advances in tracheal replacement emphasize the importance of vascularized tissue to support a viable orthotopic tracheal implant.^{41–43}

All animals in this study demonstrated evidence of graft stenosis that was associated with granulation tissue. Graft stenosis led to significant airway obstruction, requiring endoscopic intervention with stent placement to maintain airway patency (Figure 7G–J). To address chronic inflammation, modulation of the scaffold composition is critical.

The role of cell seeding in tracheal tissue engineering remains unclear. We identified that poor graft seeding correlates with earlier manifestations of respiratory distress. In tissue-engineered vascular grafts, seeded BM-MNCs prevent graft stenosis and modulate macrophage phenotype, promoting neotissue formation.^{21,44–46} Outcomes in TETGs have demonstrated less benefit: tracheal graft stenosis is not resolved by autologous cell seeding, and current cell seeding technologies have demonstrated inconsistencies that hinder outcome analyses.⁴⁷

There are several limitations to this study. First, our study represented a small cohort. Also, we did not have a control group of tracheal removal and reimplantation, which has an inherent risk of stenosis and infection.^{48,49} There are also limitations in postoperative management of airway reconstruction performed in sheep as compared with humans (inability to maintain prolonged intubation, variations in administering medication). Nevertheless, the sheep model represents a close approximation of the scale of adult tracheal replacement. Finally, although PET and PU polymers are commonly used in medical applications approved by the Food and Drug Administration, future work should expand on the testing of the cellular affinity and immunogenicity of this scaffold.⁴⁰

Conclusion

In an ovine model, synthetic TETGs previously used in humans demonstrated infectious, inflammatory, and mechanical failures that were associated with a lack of neotissue formation despite long-term implantation.

Acknowledgment

We thank the animal care and veterinary staff at The Research Institute at Nationwide Children's Hospital, Columbus, Ohio, for their support. We acknowledge the expert tissue-processing services provided by the Orthopedic Histology and Histomorphometry Laboratory at the Yale School of Medicine. Rob Strouse of Research Innovations and Solutions of The Research Institute at Nationwide Children's Hospital provided assistance in preparing illustrations.

Funding source: Funding for this study was provided from a National Science Foundation Small Business Innovation Research grant (Phase II: IIP-1456341) and the National Institute of General Medical Sciences of the National Institutes of Health (2T32GM068412-11A1 to C.A.B.).

References

1. Jungebluth P, Macchiarini P. Airway transplantation. *Thorac Surg Clin*. 2014;24:97–106. [PubMed: 24295665]
2. Elliott MJ, De Coppi P, Speggiorin S, et al. Stem-cell-based, tissue engineered tracheal replacement in a child: a 2-year follow-up study. *Lancet*. 2012;380:994–1000. [PubMed: 22841419]
3. Hamilton NJ, Kanani M, Roebuck DJ, et al. Tissue-engineered tracheal replacement in a child: a 4-year follow-up study. *Am J Transplant*. 2015;15:2750–2757. [PubMed: 26037782]
4. Elliott MJ, Butler CR, Varanou-Jenkins A, et al. Tracheal replacement therapy with a stem cell-seeded graft: lessons from compassionate use application of a GMP-compliant tissue-engineered medicine. *Stem Cells Transl Med*. 2017;6: 1458–1464. [PubMed: 28544662]
5. Gonfiotti A, Jaus MO, Barale D, et al. The first tissue-engineered airway transplantation: 5-year follow-up results. *Lancet*. 2014;383:238–244. [PubMed: 24161821]
6. Fountain H. Young girl given bioengineered windpipe dies. *New York Times* 7 7, 2013.
7. Fountain H. Christopher Lyles, got synthetic trachea, dies at 30. *New York Times* 3 7, 2012.
8. Kremer W. Paolo Macchiarini: a surgeon's downfall. <http://www.bbc.com/news/magazine-37311038?bcsi-ac-49e34401049d9f46=283EB4C700000002hZCVIAG1hhqoe+adG+t+UZegFPiISQAAAgAAAIYrfQGEAwAAAAAAAHQC8QM=>. Published September 10, 2016.
9. The Lancet. The final verdict on Paolo Macchiarini: guilty of misconduct. *Lancet*. 2018;392(10141):2
10. Warren M. UK trials of airway transplants are in limbo. *Science*. 2018;359:1448–1450. [PubMed: 29599219]
11. Clark ES, Best C, Onwuka E, et al. Effect of cell seeding on neotissue formation in a tissue engineered trachea. *J Pediatr Surg*. 2016;51:49–55. [PubMed: 26552897]
12. Pepper VK, Onwuka EA, Best CA, et al. Endoscopic management of tissue-engineered tracheal graft stenosis in an ovine model. *Laryngoscope*. 2017;127:2219–2224. [PubMed: 28349659]
13. Clark ES, Best C, Onwuka E, et al. Effect of cell seeding on neotissue formation in a tissue engineered trachea. *J Pediatr Surg*. 2016;51:49–55. [PubMed: 26552897]
14. Best CA, Pepper VK, Ohst D, et al. Designing a tissue-engineered tracheal scaffold for preclinical evaluation. *Int J Pediatr Otorhinolaryngol*. 2018;104:155–160. [PubMed: 29287858]
15. Breuer CK, Shinoka T, Snyder EL. Seeding tissue-engineered vascular grafts in a closed, disposable filter-vacuum system. *Bioprocess Int*. 2013;11:52–56.
16. Breuer C, Shinoka T, Snyder E. Seeding tissue-engineered vascular grafts in a closed, disposable filter-vacuum system. *Bioprocess Int*. 2013;11:52–56.
17. Hibino N, Nalbandian A, Devine L, et al. Comparison of human bone marrow mononuclear cell isolation methods for creating tissue-engineered vascular grafts: novel filter system versus

- traditional density centrifugation method. *Tissue Eng Part C Methods*. 2011;17:993–998. [PubMed: 21609305]
18. Kurobe H, Maxfield MW, Naito Y, et al. Comparison of a closed system to a standard open technique for preparing tissue-engineered vascular grafts. *Tissue Eng Part C Methods*. 2015;21:88–93. [PubMed: 24866863]
 19. Kurobe H, Tara S, Maxfield MW, et al. Comparison of the biological equivalence of two methods for isolating bone marrow mononuclear cells for fabricating tissue-engineered vascular grafts. *Tissue Eng Part C Methods*. 2015;21:597–604. [PubMed: 25397868]
 20. Udelsman B, Hibino N, Villalona GA, et al. Development of an operator-independent method for seeding tissue-engineered vascular grafts. *Tissue Eng Part C Methods*. 2011;17:731–736. [PubMed: 21410308]
 21. Fukunishi T, Best CA, Ong CS, et al. Role of bone marrow mononuclear cell seeding for nanofiber vascular grafts. *Tissue Eng Part A*. 2018;24:135–144. [PubMed: 28486019]
 22. Pepper VK, Francom C, Best CA, et al. Objective characterization of airway dimensions using image processing. *Int J Pediatr Otorhinolaryngol*. 2016;91:108–112. [PubMed: 27863622]
 23. Eichaker L, Li C, King N, et al. Quantification of tissue-engineered trachea performance with computational fluid dynamics. *Laryngoscope*. 2018;128:E272–E279. [PubMed: 29756207]
 24. Myer CM 3rd, O'Connor DM, Cotton RT. Proposed grading system for subglottic stenosis based on endotracheal tube sizes. *Ann Otol Rhinol Laryngol*. 1994;103:319–323. [PubMed: 8154776]
 25. Macchiarini P, Jungebluth P, Go T, et al. Clinical transplantation of a tissue-engineered airway. *Lancet*. 2008;372:2023–2030. [PubMed: 19022496]
 26. Delaere P, Vranckx J, Verleden G, De Leyn P, Van Raemdonck D. Tracheal allotransplantation after withdrawal of immunosuppressive therapy. *N Engl J Med*. 2010;362:138–145. [PubMed: 20071703]
 27. Chiang T, Pepper V, Best C, Onwuka E, Breuer CK. Clinical translation of tissue engineered trachea grafts. *Ann Otol Rhinol Laryngol*. 2016;125:873–885. [PubMed: 27411362]
 28. Fountain H. Groundbreaking surgery for girl born without windpipe. *New York Times* 4 30, 2013.
 29. Jungebluth P, Alici E, Baiguera S, et al. Tracheobronchial transplantation with a stem-cell-seeded bioartificial nanocomposite: a proof-of-concept study. *Lancet*. 2011;378:1997–2004. [PubMed: 22119609]
 30. Astakhova A. Superstar surgeon fired, again, this time in Russia. *Science*. May 16, 2017.
 31. Gilevich IV, Polyakov IS, Porkhanov VA, Chekhonin VP. Morphological analysis of biocompatibility of autologous bone marrow mononuclear cells with synthetic polyethylene terephthalate scaffold. *Bull Exp Biol Med*. 2017;163:400–404. [PubMed: 28748482]
 32. Entrican G, Wattedgera SR, Griffiths DJ. Exploiting ovine immunology to improve the relevance of biomedical models. *Mol Immunol*. 2015;66:68–77. [PubMed: 25263932]
 33. Sugiura T, Matsumura G, Miyamoto S, Miyachi H, Breuer CK, Shinoka T. Tissue-engineered vascular grafts in children with congenital heart disease: intermediate term follow-up. *Semin Thorac Cardiovasc Surg*. 2018;30:175–179. [PubMed: 29427773]
 34. Pepper VK, Clark ES, Best CA, et al. Intravascular ultrasound characterization of a tissue-engineered vascular graft in an ovine model. *J Cardiovasc Transl Res*. 2017;10:128–138. [PubMed: 28097523]
 35. Abbott WM, Megerman J, Hasson JE, L'Italien G, Warnock DF. Effect of compliance mismatch on vascular graft patency. *J Vasc Surg*. 1987;5:376–382. [PubMed: 3102762]
 36. Ballyk PD, Walsh C, Butany J, Ojha M. Compliance mismatch may promote graft-artery intimal hyperplasia by altering suture-line stresses. *J Biomechanics*. 1998;31:229–237.
 37. Deeken CR, Lake SP. Mechanical properties of the abdominal wall and biomaterials utilized for hernia repair. *J Mech Behav Biomed Mater*. 2017;74:411–427. [PubMed: 28692907]
 38. Ohno M, Fuchimoto Y, Hsu HC, et al. Airway reconstruction using decellularized tracheal allografts in a porcine model. *Pediatr Surg Int*. 2017;33:1065–1071. [PubMed: 28819688]
 39. Kutten JC, McGovern D, Hobson CM, et al. Decellularized tracheal extracellular matrix supports epithelial migration, differentiation, and function. *Tissue Eng Part A*. 2015;21:75–84. [PubMed: 24980864]

40. Maughan EF, Butler CR, Crowley C, et al. A comparison of tracheal scaffold strategies for pediatric transplantation in a rabbit model. *Laryngoscope*. 2017;127:E449–E457. [PubMed: 28776693]
41. Martinod E, Chouahnia K, Radu DM, et al. Feasibility of bioengineered tracheal and bronchial reconstruction using stented aortic matrices. *JAMA*. 2018;319:2212–2222. [PubMed: 29800033]
42. Delaere P, Lerut T, Van Raemdonck D. Tracheal transplantation: state of the art and key role of blood supply in its success. *Thorac Surg Clin*. 2018;28:337–345. [PubMed: 30054071]
43. Kolb F, Simon F, Gaudin R, et al. 4-year follow-up in a child with a total autologous tracheal replacement. *N Engl J Med*. 2018;378:1355–1357. [PubMed: 29617587]
44. Hibino N, McGillicuddy E, Matsumura G, et al. Late-term results of tissue-engineered vascular grafts in humans. *J Thorac Cardiovasc Surg*. 2010;139:431–436, 436, e431–432. [PubMed: 20106404]
45. Roh JD, Sawh-Martinez R, Brennan MP, et al. Tissue-engineered vascular grafts transform into mature blood vessels via an inflammation-mediated process of vascular remodeling. *Proc Natl Acad Sci U S A*. 2010;107:4669–4674. [PubMed: 20207947]
46. Hibino N, Yi T, Duncan DR, et al. A critical role for macrophages in neovessel formation and the development of stenosis in tissue-engineered vascular grafts. *FASEB J*. 2011;25:4253–4263. [PubMed: 21865316]
47. Maughan EF, Hynds RE, Proctor TJ, et al. Autologous cell seeding in tracheal tissue engineering. *Curr Stem Cell Rep*. 2017;3:279–289. [PubMed: 29177132]
48. Den Hondt M, Vanaudenaerde B, Verbeke E, Vranckx JJ. Requirements for successful trachea transplantation: a study in the rabbit model. *Plast Reconstr Surg*. 2018;141:845e–856e.
49. Bertolotti AM, Alvarez FA, Defranchi S, Alvarez M, Laguens RP, Favalaro RR. Successful circumferential free tracheal transplantation in a large animal model. *J Invest Surg*. 2012; 25:227–234. [PubMed: 22571688]

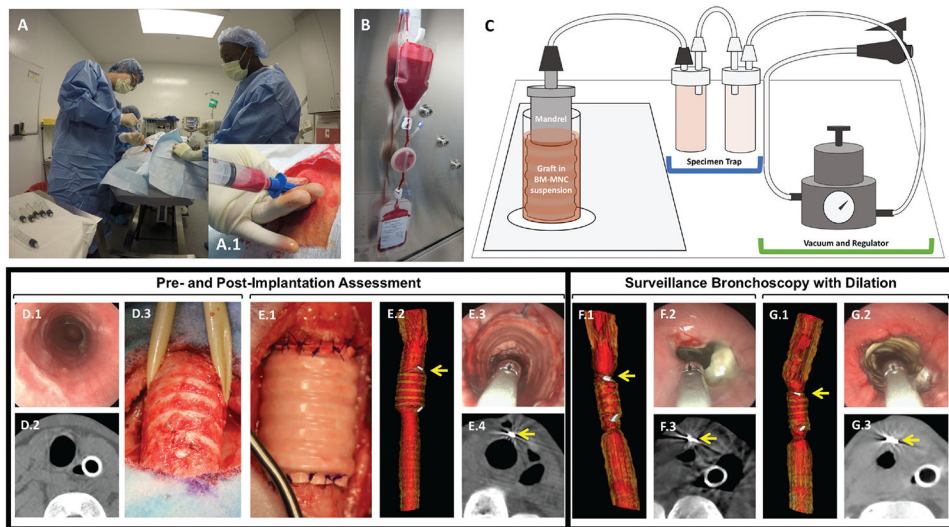


Figure 1. Lamb model of tissue-engineered tracheal graft. (A. A.1) Bone marrow harvest. (B) BM-MNC isolation. (C) Graft seeding. (D.1–3) Preimplant assessment. (E.1–3) Postimplant assessment. (F.1–3) Graft stenosis treated with graft dilation (G.1–3). Arrow: vascular clip at anastomosis. BM-MNC, bone marrow–derived mononuclear cell.

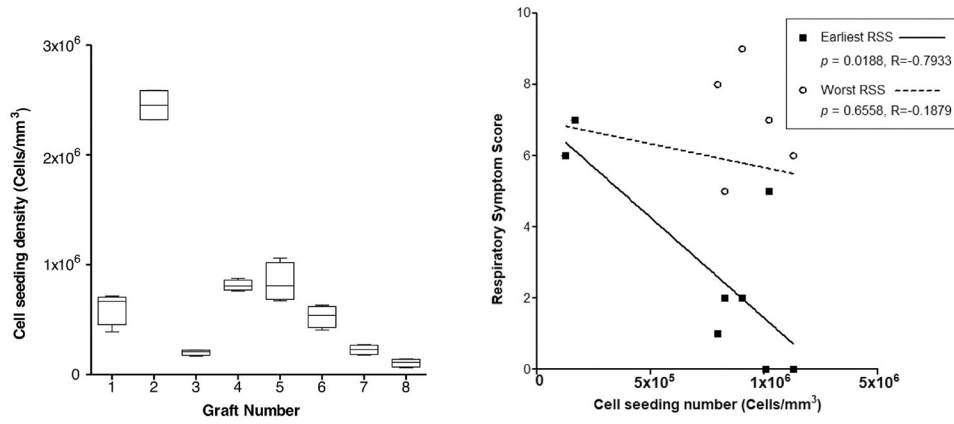


Figure 2. Graft seeding and respiratory symptoms. (A) Cell density of tissue-engineered tracheal graft scaffolds. Values are presented as box plots with median lines and minimum, maximum values. (B) Earliest and worst Respiratory Symptom Score (RSS) vs cell seeding density ($P = .0188$).

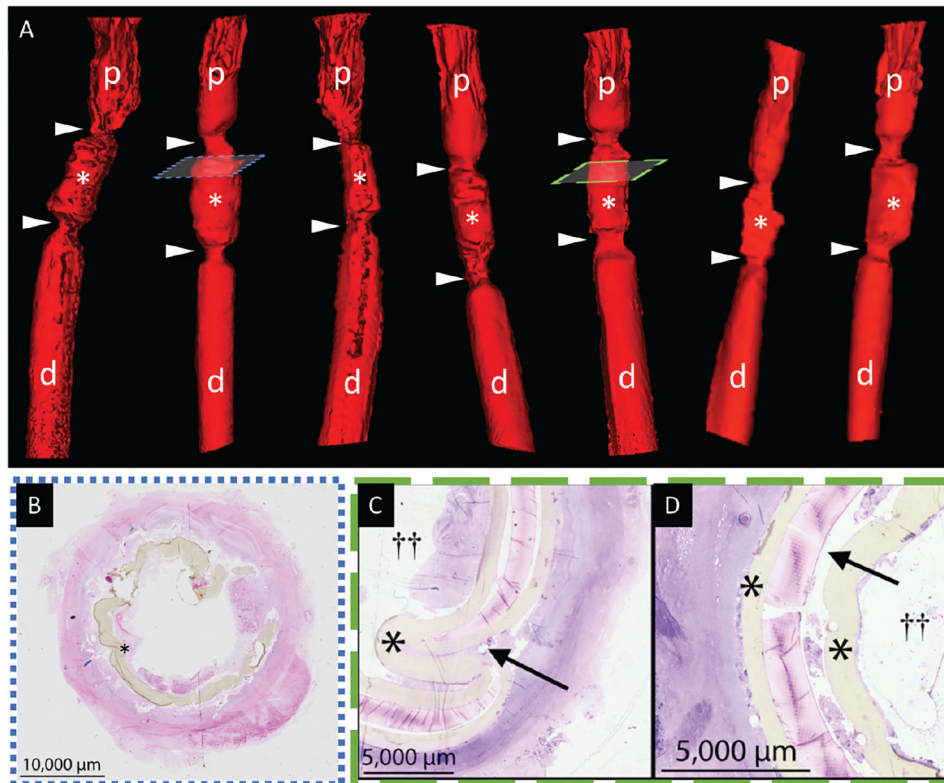


Figure 3. Graft stenosis. (A) Tissue-engineered tracheal graft prior to dilation (white asterisks). Anastomoses (arrowheads) bound by native proximal (p) and distal (d) trachea. (B) Granulation at anastomosis. (C) Posterior wall infolding (black arrow) and (D) graft delamination (black asterisk, tracheal scaffold; double cross, airway lumen).

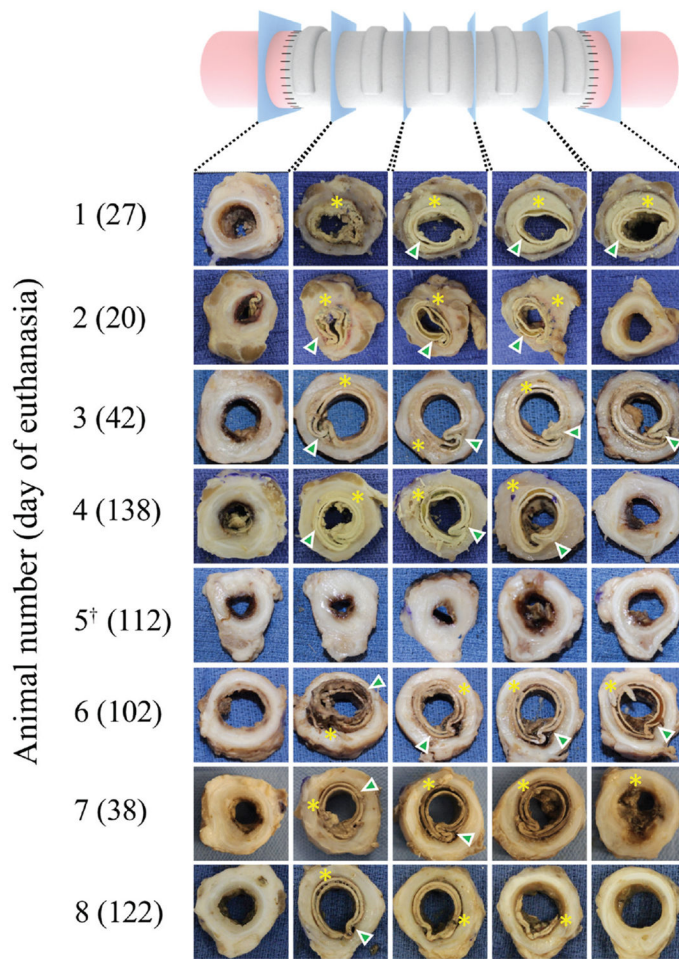


Figure 4. Gross sections of tissue-engineered tracheal graft. Encapsulation (asterisks) and graft deformation (arrowheads) in all specimens. †Indicates 1 incident of graft dislodgment.

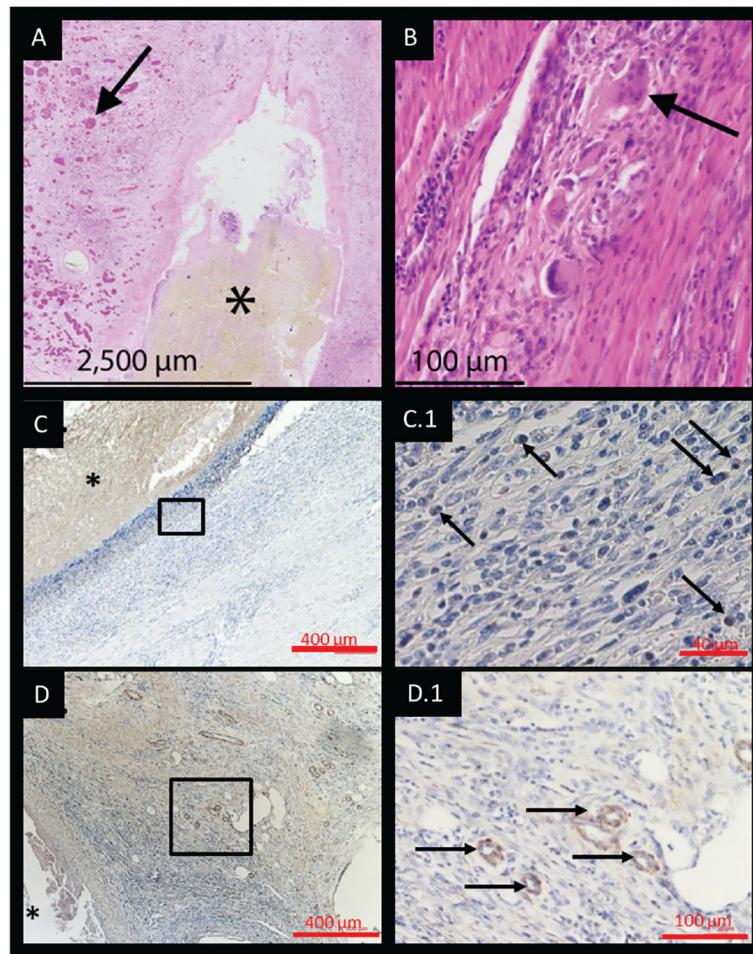


Figure 5. (A) Graft-related neotissue at the anastomosis consistent with granulation tissue (black arrows) and (B) multinucleated giant cells. (C, C.1) Macrophage (CD681) infiltration seen as well as (D, D.1) increased (α -SMA1) vascularity. Asterisks indicate tracheal scaffold; black boxes in C, D, represent high powered fields shown in C.1, D.1, respectively.

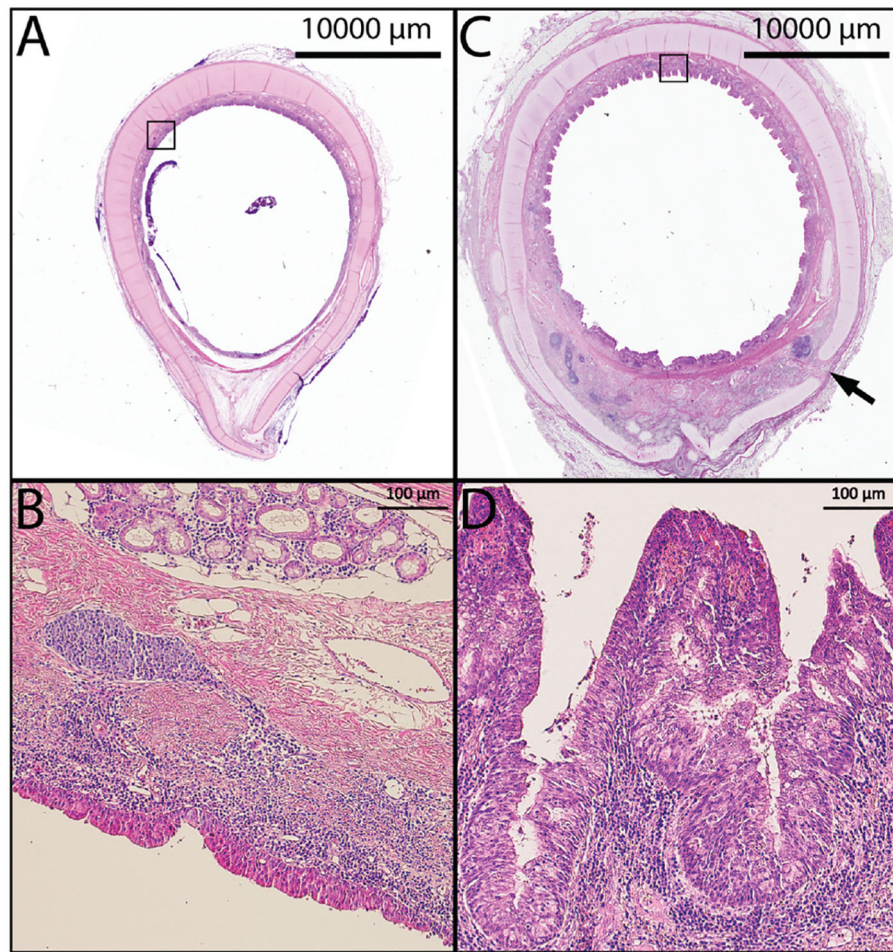


Figure 6.

(A, B) Native trachea. (C) Low-magnification axial section of the native trachea distal to the graft (day 139) showing chronic inflammation, edema, and pronounced papillary infolding. (D) Higher magnification demonstrating increased cellularity and chronic inflammation. Arrow indicates tracheal cartilage fracture from endoscopic interventions; black boxes in A, C outline high powered fields shown in B, D respectively.

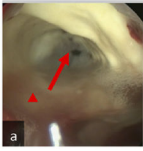
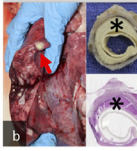
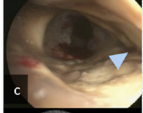

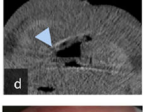
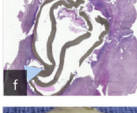

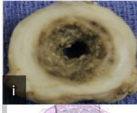
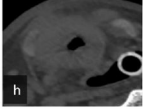
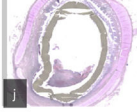
CATEGORY	PRESENTATION (incidence / 8)	SURVEILLANCE	HISTOLOGY / NECROPSY
<i>INFECTIOUS</i>	Fibropurulent exudate 8 of 8		
	Pneumonia 4 of 8		
	Lung abscess 3 of 8		
<i>MECHANICAL</i>	Posterior wall infolding 8 of 8		
	Scaffold delamination 8 of 8		
	Graft dislodgement 1 of 8		
<i>CHRONIC INFLAMMATORY</i>	Graft stenosis 8 of 8		
	Granulation tissue 8 of 8		

Figure 7. (A) Purulence (red arrowhead, arrow). (B) Lung abscess (red arrow), fibropurulent exudate (*) in gross section and histology (upper, lower inset). (C) Posterior wall infolding (blue arrowhead). (D-F) Scaffold delamination. (G-J) Graft stenosis.

Table 1.

Summary of Implants.

	Animal								Mean ± SD and Summary
	1	2	3	4	5	6	7	8	
Preimplant weight, kg	40.5	34.4	41	55	53.5	47.5	27.5	28.5	41 ± 10.5 kg
Native trachea diameter, mm	17.4	18.2	16.3	17.4	14.9	18.2	14	16.3	16.6 ± 1.5 mm
POD of first respiratory distress symptom	27, W	20, none	16, S	25, S	17, S	9, S	12, S	18, S	18 ± 7 d, S (6), W (1)
POD of first bronchoscopy	27	20	20	22	21	20	15	14	20 ± 4 d
Location of maximal stenosis	P	D	P	D	D	D	D	D	Distal (6), proximal (2)
CM grade (I-IV), % maximal stenosis	III, 80	III, 83	II, 66	II, 70	I, 46	III, 81	III, 81	III, 79	73 ± 12.5
Stent placed during surveillance	No	No	Yes	Yes	Yes	Yes	Yes	Yes	Stented (6)
Surveillance bronchoscopies performed, n	1	1	2	5	4	4	3	4	—
Planned endpoint	6 wk	6 wk	6 wk	4 mo	4 mo	4 mo	4 mo	4 mo	4 mo (5), 6 wk (3)
Euthanasia date, POD	27	20	42	138	112	102	38	122	—
Cause of death	G	A, L	E	E	E	G	A	E	E (4), A (2), G (2), L (1)
Graft epithelialization	No	No	No	No	No	No	No	No	None

Abbreviations: A, anesthesia related; CM, Cotton-Myer; D, distal; E, endpoint met; G, graft related; L, lung abscess; P, proximal; POD, postoperative day; S, stridor; W, wheeze.